ROYAL SOCIETY OPEN SCIENCE

rsos.royalsocietypublishing.org

Research

Article submitted to journal

Subject Areas:
mathematical modelling, epidemiology, infectious diseases

Keywords:
COVID19,mathematical modelling, social distancing, healthcare burden, cost analysis, testing impact

Author for correspondence:
I. R. Moyles
e-mail: imoyles@yorku.ca

Cost and social distancing dynamics in a mathematical model of COVID-19 with application to Ontario, Canada

I. R. Moyles[1,2], J. M. Heffernan[1,2] and J. D. Kong[1,2]

[1]Department of Mathematics and Statistics, York University, Toronto, Canada
[2]Centre for Diseases Modeling (CDM), York University, Toronto, Canada

A mathematical model of COVID-19 is presented where the decision to increase or decrease social distancing is modelled dynamically as a function of the measured active and total cases as well as the perceived cost of isolating. Along with the cost of isolation, we define a healthcare cost and a total cost. We explore these costs by adjusting parameters that could change with policy decisions. We observe that minimum costs are not always associated with increased spending and increased vigilance which is due to the desire for people to not distance and the fatigue they experience when they do. We demonstrate that an increased in the number of lock-downs, each of shorter duration can lead to minimal costs. Our results are compared to case data in Ontario, Canada from March to August 2020 and details of extracting the results to other regions is presented.

1. Introduction

As of early October 2020 there have been over 33 million cases of COVID-19 worldwide, over 150 000 cases in Canada, and over 50 000 cases in the province of Ontario. The early stages of the outbreak focused on mathematical modelling of disease dynamics such as transmission and the basic reproduction number [1,2]. It quickly became clear that asymptomatic spreading was important and that undetected infections were important to consider in models [14].

© 2014 The Authors. Published by the Royal Society under the terms of the Creative Commons Attribution License http://creativecommons.org/licenses/by/4.0/, which permits unrestricted use, provided the original author and source are credited.

THE ROYAL SOCIETY PUBLISHING

This caused a global policy shift towards travel restrictions, community closures, and social distancing implementations. The impacts of mathematical modelling on policy are documented in [20].

The implementation of non-pharmaceutical intervention (NPI) such as social distancing quickly became an important mathematical modelling task (cf. [16,17,19,31]). The majority of these models focus on fixed policy implementations such as reducing contacts on a given date and reinstating them on another. There are two main issues with this, the first is that it requires knowledge of the implementation and relaxation times. While this can be explored in model simulations and optimized for best results, its independence from the model itself can make it hard to adapt to other diseases, strains, or important factors. A second problematic issue is that it assumes a instantaneous policy compliance, i.e., that people will immediately reduce contacts upon implementation and stop upon relaxation. While this can be impacted by an adherence parameter, it does not allow for a dynamic response which is more realistic of human choice. Therefore a dynamics social distancing model that reacts to the disease dynamics is more realistic.

A dynamic intervention strategy where intervention was turned on and off based on the state of the epidemic was considered in [31] where a decrease in both total infections and social distancing duration was observed compared to a fixed-duration intervention which they also considered. However, modelling the dynamics of intervention entirely on the disease progression assumes that people will immediately distance or relax at some threshold. This suggests that a periodic solution will emerge centered around the critical disease threshold and this appears to happen in [31]. While it is quite realistic that disease dynamics drive people into isolation, it is a separate mechanism, namely the cost of staying home, that people consider when relaxing their isolation habits. Cost is seldom considered in models, with most of the focus on larger economic influence [4,22]. These economic factors certainly play a role in individual cost but psychological factors such as loneliness and habit displacement are important as well

For this paper we propose a differential equation model for the spread of COVID-19 with separate dynamics for isolation and relaxation dependent on disease progression and relaxation cost respectively. The disease progression information typically comes from media reports and has been investigated in the context of infectious diseases such as influenza (cf. [7,8,30,33]) and is usually used to reduce the susceptibility of individuals who are positively influenced by media. The relaxation cost is less often considered and its inclusion recognizes that repeated lock-downs would have diminishing returns as the cost to stay home becomes too overwhelming. A dynamic response model allows for more realistic policy strategies for disease mitigation and mortality prevention. Our model focuses on the spread of the disease in Ontario, Canada, but could be adapted with other parameters to other regions.

Our study is outlined as follows. In section 2 we introduce the model and the dynamic response functions for social distancing and relaxation. We also introduce the parameters including those which we fit to data from [25]. We define health, economic, and total costs of the pandemic. The health cost is based on overloading existing healthcare resources while the economic cost is the personal or societal cost of social distancing. We show the excellence of fit to our data in section 3 and present a series of results based on different scenarios where policy parameters that control distancing and relaxing are varied. We consider scenarios where both health and relaxation costs are equally weighted or where health cost is much more strongly influencing the total cost. We consider a modification to the relaxation rate so that it depends on both cost and cases and see that multiple outbreak peaks can occur. We discuss the implications and conclusions of our work in section 4.

2. Model

We consider a mathematical model for COVID19 consisting of classes of people with various exposure to the disease. These classes are listed in Table 1where we note that the removed groups include people who have died from the virus which we do not separately consider. For each of the

population classes we assume there are three levels of social distancing indicated by a variable subscript zero, one, or two. If the subscript is 0 then there is no social distancing, subscript 1 indicates that there is social distancing which reduces the contact probability by some percentage while for subscript 2, the contact probability is zero, i.e. full isolation. We introduce a further subscript, M which represents the mitigation on spread due to individuals who have tested positive and are isolated. We assume that only P, I_S, and I_A populations can test positive and that these people will immediately and completely isolate effectively placing them in the social distance 2 category for the duration of their disease.

We follow the usual SEIR model framework (cf. [13,15]) which we illustrate in Figure 1 with equations detailed in Appendix A.

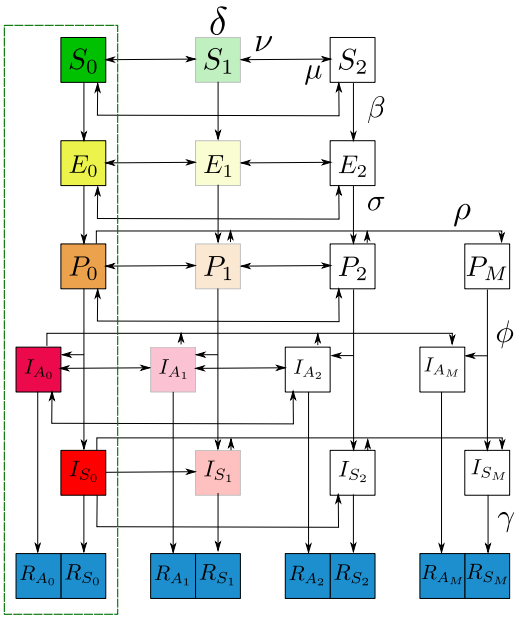

Figure 1: Graphical representation of the SEIR model used throughout the manuscript. The fading colours indicates a reduction in transmission due to distancing or isolation. The portion of the model in the green rectangle is the model when social distancing and testing is not considered

For the model we assume that vital statistics are not important on the time scales we consider so we take a fixed population N. We also normalize the model by another population N_{crit} which is the amount of people needing healthcare resources that puts the system at full capacity. Figure 1 also shows the various model parameters which are summarized in Table 1. Each transition parameter has a subscript (i, j) with i the originating class and j the terminal class. The exception to this is $\beta_{i,j}$ where i is the class of the susceptible person and j the class of the infected contact. Whenever there are multiple paths for a class, a parameter $q_i \in [0, 1]$ is used to partition them into each final compartment.

We make the following assumptions about the model parameters:

(i) the parameters δ, σ, ϕ, γ, and q_i are constant and the same for each social distancing class as the disease progression characteristics are unaffected by social distancing.

Table 1: Variable and Parameter Definitions

	Definition	Value	Comment
S	Susceptibles, people who can catch the virus	$0.9998N$	Initial Condition
E	Exposed, people who have caught the disease but are not yet infectious	0	Initial Condition
P	Pre-symptomatic, people who are infectious but have not had the disease long enough to show symptoms	0	Initial Condition
I_S	Infected-symptomatic, people who are infectious and have started showing symptoms	$2 \times 10^{-4} N$	Initial Condition
I_A	Infected-asymptomatic, people who are infectious but never show symptoms	0	Initial Condition
R_S	Removed-symptomatic, people who were symptomatic and infectious, but are no longer infectious	0	Initial Condition
R_A	Removed-asymptomatic, people who were asymptomatic and infectious, but are no longer infectious	0	Initial Condition
N	Population of Ontario	13448494	2016 Census
N_{crit}	Critical population at which healthcare resources are overwhelmed	81301	Chosen
R_0	Basic reproduction number	2.4	[10,24]
β	Transmission rate of disease after coming in contact with the infected class	$0.223\ \text{d}^{-1}$	See (2.9)
δ	Reduction in transmission due to social distancing in class 1	0.25	Chosen
α	Reduction in transmission due to being asymptomatic	0.50	Chosen
σ	Rate at which exposed class enter pre-symptomatic class	$2\ \text{d}^{-1}$	[10]
ϕ	Rate at which pre-symptomatic class can beging showing symptoms	$4.6^{-1}\ \text{d}^{-1}$	[5,10,11]
q	Proportion of infected individuals who show symptoms	0.69	Median value
γ	Rate at which an infected person is no longer infectious	$10^{-1}\ \text{d}^{-1}$	[32]
$\mu_{\max}$	Maximal rate at which someone moves from a less socially distant class to a more socially distant class	$1\ \text{d}^{-1}$	Chosen
$\mu_{\max}$	Maximal rate at which someone moves from a more socially distant class to a less socially distant class	$1\ \text{d}^{-1}$	Chosen
μ_I	Rate at which people showing symptoms choose to isolate	$0.01\ \text{d}^{-1}$	Chosen
q_0	Proportion of S_0 socially distancing into S_1	0.9	Chosen
q_2	Proportion of S_2 relaxing social distancing into S_1	0.6	Chosen
q_I	Proprotion of symptomatic individuals I_{S0} who isolate into I_{S1}	0.6	Chosen
ρ_A	Testing rate for someone not showing symptoms to test positive	$8.7 \times 10^{-3}\ \text{d}^{-1}$	See Appendix B
ρ_S	Testing rate for someone showing symptoms to test positive	$3.48 \times 10^{-2}\ \text{d}^{-1}$	See Appendix B
M_c	Critical active cases to induce social distancing	$2090/N_{\text{crit}}$	See Appendix B
M_0	Active cases that leads to half the maximal rate of social distancing	$4180/N_{\text{crit}}$	See Appendix B
k_c	Critical approximate disease doubling rate to induce social distancing	$16.24^{-1}\ \text{d}^{-1}$	See Appendix B
k_0	Approximate disease doubling rate that leads to half the maximal rate of social distancing	$4.06^{-1}\ \text{d}^{-1}$	See Appendix B
C_c	Critical cost to induce social relaxation	50 d	Chosen
C_0	Cost that leads to half the maximal rate of social relaxation	100 d	Chosen

(ii) $\beta_{S_0 I_{S_0}} = \beta$ a constant which incorporates both contact and disease transmission probability. We assume that people not showing symptoms shed a lower viral load and hence reduce transmission by a constant factor α and that those in social distancing class 1 reduce their contacts by a constant factor of δ, effectively also reducing their transmission. For example $\beta_{S_0 I_{A_0}} = \alpha\beta$, $\beta_{S_1 I_{S_0}} = \delta\beta$, and $\beta_{S_1 I_{A_1}} = \alpha\delta^2\beta$.

(iii) people in the infected symptomatic class I_{S_0} choose to isolate at a constant rate μ_I with q_I going into I_{S_1} and $(1 - q_I)$ going into I_{S_2}. They stay in the social distancing class until they have recovered from the disease, i.e., $\nu_I = 0$. Furthermore, this means that someone

already social distancing in state 1 or 2 who becomes symptomatic remains in that social distance class. We note that individuals in I_{S_0}, I_{S_1}, and I_{S_2} know that they are sick but have not tested positive for the disease. If they test positive, they transition to I_{S_M} and are completely quarantined.

(iv) there are two testing rates ρ_A and ρ_S for asymptomatic (including presymptomatic) and symptomatic individuals respectively with $\rho_S > \rho_A$ as we assume that symptomatic people are more likely to seek out a test as they would have symptoms. Asymptomatic people are likely to only seek a test out of curiosity or if they have been in contact with someone who has tested positive. Despite the fact that testing numbers fluctuate with the progression of the disease we take the testing rates to be constant which makes them an effective average testing rate. This is consistent with studies estimating global infections per symptomatic test case (cf. [18,26]). To help restrict the model we take $\rho_S = 4\rho_A$ which is a similar value as observed in [18] who compared data to Germany, South Korea, and the USA.

(v) we assume that only people in the P, I_S or I_A classes will test positive if a test is administered. Therefore, we explicitly assume people in the E class do not have a high enough viral load to shed.

(vi) people who have tested positive are isolated (effectively put in social class 2) until recovery and cannot transmit the disease. This ignores infections to family members living in a household with an isolated member or infections to healthcare workers who are conducting tests or treating COVID-19 patients. See [34] for considerations of a model with household structure included.

(a) Social Distancing and Testing

Since people without symptoms are unaware of whether they have the virus or not, we assume that both social distancing and relaxing rates are independent of the disease class they are in. We therefore define μ as the rate of social distancing from state 0 with proportion q_0 going to state 1 and $(1 - q_0)$ going to state 2. We similarly define ν as the rate of decreasing social distance from state 2 with proportion q_2 going to state 1 and $(1 - q_2)$ going to state 0. We define those social distancing from state 1 to state 2 as $\mu/2$ to account for the fact that anybody in state 1 has already undergone one transition and so they should be slower at making a secondary transition. For a similar reason we define the social distancing relaxation from state 1 to state 0 as $\nu/2$.

Testing provides two important quantities reported by the media that can help inform social distancing, the total number of cases M and the active cases M_A (each also scaled by N_{crit}) which are defined by

$$\dot{M} = \rho_S(I_{S_0} + I_{S_1} + I_{S_2}) + \rho_A(I_{A_0} + I_{A_1} + I_{A_2} + P_0 + P_1 + P_2), \tag{2.1a}$$

$$M_A = P_M + I_{S_M} + I_{A_M}. \tag{2.1b}$$

If the disease is in the exponential phase of spread then the doubling rate can be deduced from the cumulative case information, M, to yield

$$k_M = \frac{\frac{\mathrm{d}M}{\mathrm{d}t}}{M \ln 2}. \tag{2.2}$$

We assume that this can approximate the doubling rate at all times and is what locally drives social distancing. However, while the disease growth rate is important, it should be weighed against the number of active cases as well and therefore we propose a social distance transition function

$$\mu = \mu_{\max} \left(\frac{[k_M - k_c]_+}{[k_M - k_c]_+ + k_0 - k_c} \right) \left(\frac{[M_A - M_c]_+}{[M_A - M_c]_+ + M_0 - M_c} \right), \tag{2.3}$$

where $\mu_{\max}$ is the maximal rate of social distancing, $[\cdot]_+$ is defined such that,

$$[\cdot]_+ = \max(\cdot, 0).$$

Social distancing is not something that people want to do and the parameters k_c and M_c represent critical doubling rates and active case numbers respectively below which people will not social distance which is the role of the maximum function. These parameters can be thought of as policy parameters since implementing lock-downs, closing businesses, and halting social gatherings will impact these values. The parameters k_0 and M_0 represent doubling rates and case numbers where social distancing reaches its half-maximum.

We assume that social relaxation, ν, is proportional to the cost of social distancing, C. This may be economic cost in the form of people staying home from their jobs, but also the psychological cost of being isolated for a long period of time. We model the cost as,

$$\dot{C} = \frac{N_{\text{crit}}}{N}\left((S_2 + E_2) + (1-\delta)(S_1 + E_1)\right), \tag{2.4}$$

where we only include susceptible and exposed classes because we assume there is a greater benefit to having transmitting classes (P_i, I_i) stay home. Arguably, exposed people who will soon become infectious should stay home too, but as they would test negative, they would think they are healthy and therefore we assume they contribute to the cost. For simplicity we ignore the cost of recovered people social distancing which will be invalid if many people have recovered but policy prevents them from returning to their workplaces etc. As written, the cost accumulates with time. We could remedy this by including a decay factor $-\mu_C C$ in (2.4) but we assume that the time scale of recovery is much longer than that of the pandemic. Since the cost does not factor in day-to-day economic costs in non-pandemic times, it is normalized so that zero cost represents the cost of society pre-pandemic. Similarly then the maximum additional costs come from those isolating completely in social distance state 2. Those in social distance state 1 effect their transmissibility by a factor δ and we assume this comes at a reciprocal burden cost of $(1-\delta)$. For example, if $\delta = 1$ then the 1 and 2 states are both fully isolated and contribute an equal maximal cost. We note that since populations are non-dimensional in the model, the cost is denoted in days where one day represents the cost of every person being in social distance state 2.

Defining the cost, we propose ν be modelled by

$$\nu = \nu_{\max}\frac{[C - C_c]_+}{[C - C_c]_+ + C_0 - C_c} \tag{2.5}$$

where $\nu_{\max}$ is the maximal rate at which social distancing can be relaxed, C_0 is the cost which triggers the half-maximal rate, and C_c is the cost required to trigger social relaxation. C_c is also a policy parameter as mental health promotion, economic stimulus, and wage subsidy programs can influence the cost people can endure before social relaxation.

To understand the true cost of the pandemic we must balance the relaxation cost, C, with the healthcare cost, H, which we define as

$$H = \sum_i \int_{t_{0_i}}^{t_{1_i}} M_A \, \mathrm{d}t, \tag{2.6}$$

where t_0 is the time where active cases begin to strain the healthcare system and t_1 is the time they stop. This measures the burden on the healthcare system, and likely on mortality rates, if active cases get too large. We have defined N_{crit} as the value above which healthcare resources are exceeded and we assume the burden on the system begins when $N_{\text{crit}}/2$ is reached. The choice of defining H balances intensity of the outbreak along with duration. The sum allows for multiple outbreaks where the hospital resources are exceeded. The reason we measure active cases is that we assume all COVID-19 cases entering the hospital will be tested. Realistically a portion of the untested symptomatic cases will also exasperate the healthcare system and therefore this can be considered an underestimated cost. Having defined the healthcare cost we can then define the total cost as

$$C_T = \omega\frac{H}{H_\infty} + (1-\omega)\frac{C}{C_\infty}, \tag{2.7}$$

where H_∞ is the healthcare cost with no social distancing intervention ($\mu_{\max} = 0$) and C_∞ is the largest isolation cost allowable. We define ω as a weighting factor between the two cost contributions. In the absence of actual dollar amounts, the total cost as defined in (2.7) is a relative cost.

(b) Parameter Determination

We first consider a variant of the full model that does not include social distancing or testing (green-dash rectangle of Figure 1) which is given by,

$$\begin{aligned}
\dot{S} &= -\frac{N_{\text{crit}}}{N}\left(\beta_{SP}SP + \beta_{SI_S}SI_S + \beta_{SI_A}SI_A\right)\\
\dot{E} &= \frac{N_{\text{crit}}}{N}\left(\beta_{SP}SP + \beta_{SI_S}SI_S + \beta_{SI_A}SI_A\right) - \sigma E\\
\dot{P} &= \sigma E - \phi P\\
\dot{I}_S &= q\phi P - \gamma_S I_S\\
\dot{I}_A &= (1-q)\phi P - \gamma_A I_A\\
\dot{R}_S &= \gamma_S I_S\\
\dot{R}_A &= \gamma_A I_A.
\end{aligned} \tag{2.8}$$

This reduced model represents the disease transmission dynamics prior to widespread knowledge of COVID-19. Following [10] we assume that people without symptoms are half as infectious as those with symptoms and therefore take $\alpha = 1/2$.

The disease free state is $[S, E, P, I_S, I_A, R_S, R_A] = [N/N_{\text{crit}}, 0, 0, 0, 0, 0, 0]$ and we identify the basic reproduction number R_0 as the non-zero eigenvalue of the next generation matrix produced from (2.8) (cf. [9,12]),

$$R_0 = \frac{\beta(\gamma_S\gamma_A + 2q\phi\gamma_A + \phi\gamma_S(1-q))}{2\phi\gamma_S\gamma_A}. \tag{2.9}$$

Taking R_0 from measurements such as the studies in [10,24] which estimate $R_0 = 2.4$ we can rearrange (2.9) to determine a value for β.

We assume that this base transmission rate between the susceptible and symptomatic populations is the same as that between S_0 and I_{S_0} in the social distancing model (A 1), i.e. $\beta_{S_0 I_{S_0}} = \beta$. The parameters considered for the base model are presented in Table 1 and we comment on some of the assumptions made.

As of July 16, 2020, the hospitalization rate of COVID-19 in Ontario Canada was 12.3% and there were approximately 10000 hospital beds available for people which together define $N_{\text{crit}} = 81301$. We choose $\mu_{\max} = \nu_{\max} = 1$ under the assumption that people generally need at least one day to change their routines. We arbitrarily assume that $C_0 = 2C_c$ and that $k_0 = 4k_c$ to help constrain the model. This means that the relaxation cost needed to initiate the half-maximum rate is twice as many days as the onset of social relaxation while the disease needs to double twice for the half-maximal social distancing rate to occur. We chose $C_c = 50$ based on Ontario imposing a stage-one lock-down that lasted almost 100 days with the fact that it did not impact the entire province.

We predicted the values of k_c, M_c, and ρ_A (recalling that $\rho_S = 4\rho_A$) by fitting our model to active and total case data from [25] between March 10, 2020 August 18, 2020 inclusive. We used a non-linear least squares method for the fitting, the details of which are in Appendix B. Using the N_{crit} scale we can convert the values of M_c and M_0 from Table 1 to 2090 and 4180 people respectively. The values of μ_I, q_0, q_2, and q_I are arbitrarily chosen. However, as is seen in Appendix B where a sensitivity analysis is performed, these parameters are not very influential on model results so their values are not likely very consequential on model results. The most influencing parameter is μ_I. Considering that at the half-maximal rates, the social distancing rate is $\mu = 1/4$ and that a recent study from [3] suggested that up to 90% of Americans go into work

sick then a further 90% reduction would yield $\mu_I \approx 0.025$ which is the same order of magnitude to the chosen value.

We took a median value for the symptomatic rate of 69% following a variety of studies (see [6,21,23,27–29]).

3. Results

We simulated (A 1) using MATLAB 2020a with parameters in Table 1. We took March 10, 2020 as the initial time with an initial condition that 0.02% of the population was infected with symptoms and placed the remaining 99.98% of the population in the susceptible class.

We demonstrate the results from data-fitting the parameters k_c, M_c, and ρ_A in Figure 2. Comparing data to simulation, we observe a difference in the early peak-time of 4.7 days and a difference in peak active cases of 359 people.

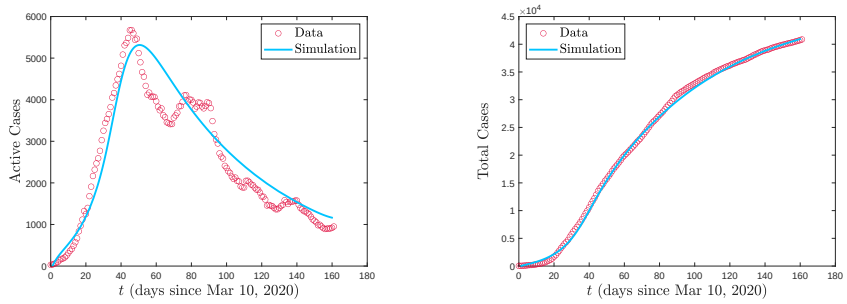

(a) (b)

Figure 2: Comparison between simulation and data from [25] from March 10 to August 18, 2020.

We observe the impact of the disease on total cost (2.7) by simulating the full model (A 1) and varying the critical threshold at which people social distance (M_c) and the critical cost before social relaxation begins (C_c). We consider 1/4, 1/2, 2, and 4 times the base values given in Table 1. The value for k_c from data fitting is already quite extreme and we do not vary this. We plot heat maps for H, C, and C_T given by (2.6), (2.4), and (2.7) respectively in Figure 3 where they are coloured relative to the maximal and minimal costs. We compute H_∞ by simulating the model with parameters in Table 1 and taking $\mu_{\max} = 0$. We take C_∞ as the highest cost that emerges from all of the simulations. Intuitively this occurs at $M_c = M_c^*/4$ and $C_c = 4C_c^*$ as evidenced in Figure 3b. We consider an even weighting between H and C ($\omega = 1/2$) in Figure 3c as well as a 90:10 $H : C$ weighting ($\omega = 0.9$) in Figure 3d.

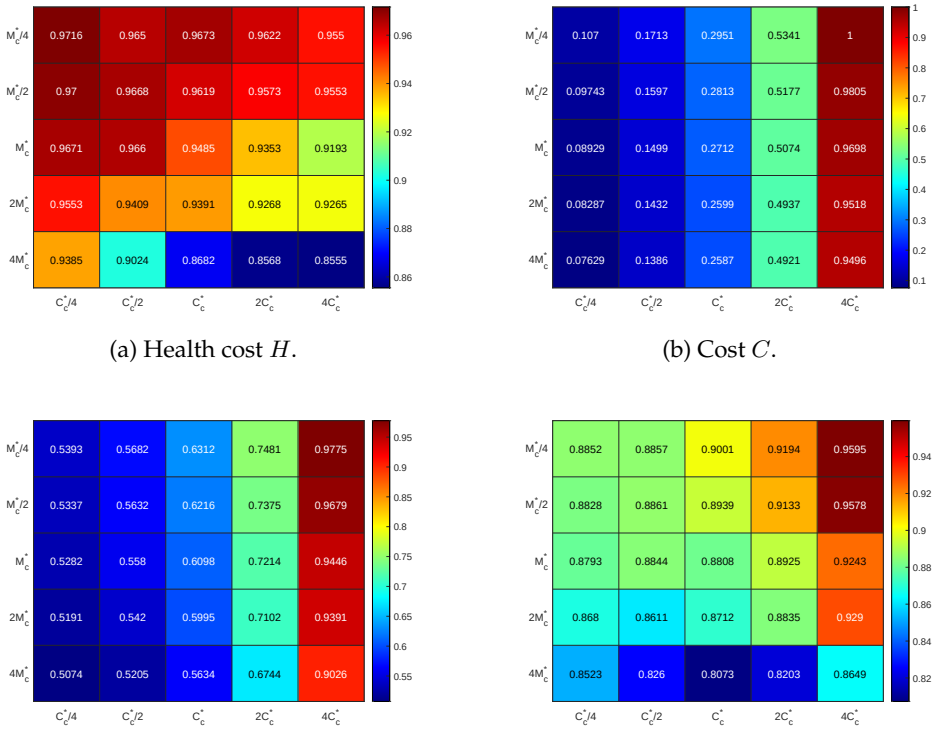

(a) Health cost H.

(b) Cost C.

(c) Total cost C_T (50/50 weighting).

(d) Total cost C_T (90/10 weighting).

Figure 3: Health, cost, and total cost from varying M_c and C_c in the model (A 1) with other parameters fixed from Table 1 (excluding k_0 and M_0 which are appropriately updated). M_c^* and C_C^* refer to the base values in Table 1. In these simulations $H_\infty = 292.7$ and $C_\infty = 230$ days.

The overall trend, particularly with even weighting, is unsurprising, namely that increased vigilance (larger M_c) and increased spending (larger C_c) contribute to a larger cost. However, there are some important things to note. Firstly, this trend is not always true. For example in Figure 3a at $M_c^*/4$, the health cost increases when transitioning from $C_c^*/2$ to C_c^*, i.e. doubling the critical cost allowing people to stay home longer, causes a worse health outcome. We plot the active cases for these two scenarios in Figure 4 where we see that indeed spending more adds a delay to the peak time and decreases the peak value, but the duration above the critical health threshold of $N_{\text{crit}}/2$ is three days longer. This added time impact leads to a larger overall health cost.

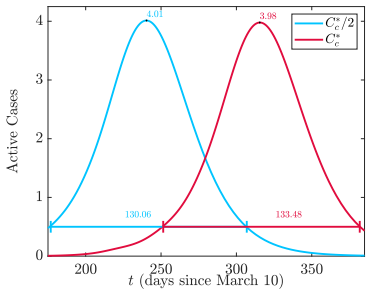

Figure 4: Comparison of the cases for $C_c^*/2$ and C_c^* with $M_c = M_c^*/4$ from Figure 3a. We note the peak value at C_c^* is less than $C_C^*/2$ but the duration of time above the critical threshold of $N_{\text{crit}}/2$ is longer.

A second interesting feature of note in the health cost is that the decision of whether to increase vigilance or the critical cost is not always clear. For example if the vigilance is at $2M_c^*$ and the cost at $C_c^*/4$ in Figure 3a then it is more beneficial (less relative health cost) to double vigilance than to double critical cost. However starting at M_c^* and C_c^* it is more beneficial to double critical cost than double vigilance. An extreme example is at $M_c^*/4$ and $C_c^*/2$ where doubling either critical cost or vigilance each lead to higher healthcare costs. This is important to note from a policy standpoint because it can look like both policy initiatives are failures, however it is only stating that the improvement measures were not sufficient enough and more needs to be done. For example quadrupling the critical cost does reduce the healthcare cost. This same non-uniform decision process is not true for social relaxation cost, C, as spending more always increases the cost and increasing vigilance always decreases the cost. This trend persists for the total cost when both are equally weighted, however in the 90/10 weighting, a weighting that may be more consistent with prioritizing human lives, a richer structure emerges. For example, in Figure 3d starting at M_c^* and C_c^* it is more costly to both half and double spending indicating that an optimal spending level is met at that vigilance. As well, at M_c^* and $4C_c^*$ it is more costly to both double and half vigilance indicating a optimal vigilance balance there. The global minimum in the parameter space considered is at C_c^* and $4M_c^*$ where decreasing vigilance as well as increasing or decreasing critical cost leads to overall more costly outcomes. Non-uniform trends and local minima in costs are important considerations that should be made in policy decisions.

A third important feature to recognize in Figure 3 is that even when intuitive trends of cost increases are followed, the relative increase in cost can be quite different. For example in Figure 3d starting at M_c^* and C_c^* doubling the critical cost is a 1.3% increase in total cost but doubling the critical cost again is a 3.6% increase in total cost. For Figure 3c starting at a high vigilance of $4M_c^*$ with C_c^* and doubling critical cost results in a 19.7% increase in total cost, but doubling it again results in a 33.8% increase in total cost. A lower relative increase in cost indicates that the strategy was more effective compared to others.

Plots of all of the active cases and costs for the scenarios in Figure 3 can be found in the supplementary material. The cumulative number of symptomatic-infected people for each scenario is plotted in Figure 5.

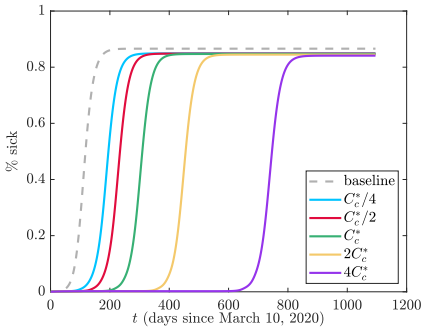

(a) $M_c^*/4$.

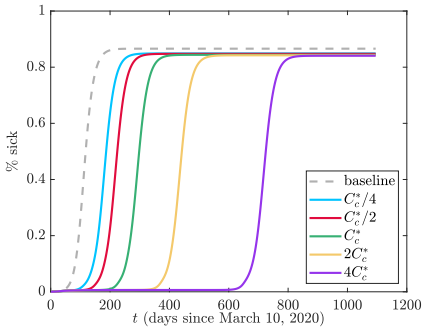

(b) $M_c^*/2$.

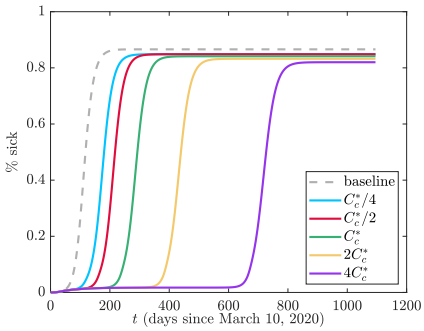

(c) M_c^*.

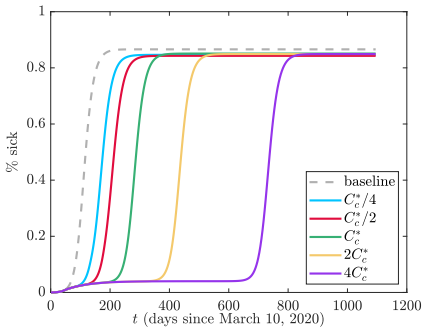

(d) $2M_c^*$.

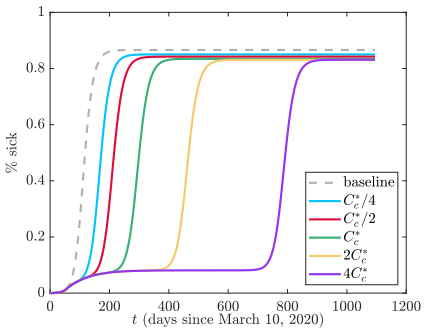

(e) $4M_c^*$.

Figure 5: Total cumulative symptomatic cases (plotted as a percentage of the total population). The baseline case refers to no social distancing, i.e. $\mu_{\max} = 0$.

It can be seen that decreasing vigilance causes a more uniform accumulation of cases while increasing relaxation cost delays the peak of infection. In all cases, the same number of total people are infected as in the baseline case where testing occurs but no social distancing happens. This is expected as complacency and fatigue from non-pharmaceutical interventions eventually force the cost of social distancing to be too high for people to remain away from others. However, these delays can provide time for vaccination and other medical efforts to minimize the impact of the disease.

(a) Multiple Secondary Waves

The model as derived only allows for one large secondary wave following the peak in Ontario around early May 2020. Since the relaxation rate ν is solely a function of relaxation cost (2.4) which is always increasing, isolation fatigue becomes too overwhelming that there is resistance for entering secondary lock-downs. This model is likely appropriate for regions that have a strong aversion to social distancing. For other regions, it is likely that relaxation will be a function of cost and active cases as people will prioritize their health in a sustained outbreak and thus not want to relax if case numbers are sufficiently large. If we refer to the rate in (2.5) as ν_0 then we propose modifying ν to

$$\nu = \nu_0 \left[\eta M_c - M_A\right]_+ , \tag{3.1}$$

where η is the factor of critical cases M_c that stops social relaxation regardless of cost. Implementing this change allows for secondary infection peaks as evidenced in Figure 6 where we use parameters in Table 1 and arbitrarily take $\eta = 1/2$ for Figure 6a and $\eta = 1/5$ for Figure 6b. It is important to note that these changes do not impact the initial peak fitted to data in Figure 2 and only alter future projections. For this reason, it is difficult to estimate η as several peaks will need to have occurred.

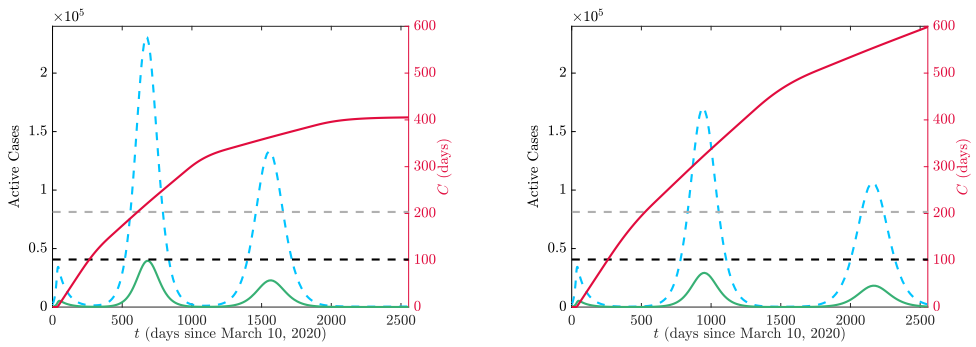

(a) $\eta = \frac{1}{2}$. (b) $\eta = \frac{1}{5}$.

Figure 6: Comparison of true active cases (dashed blue), tested active cases (solid green), and cost (solid red) for two values of η. The grey-dashed line is the hospital resources N_{crit} and the black-dashed line is $N_{\text{crit}}/2$ from which the health cost is measured.

We repeat the cost analysis as in Figure 3 for the modified relaxation cost (3.1), however we fix $M_c = M_c^*$, the value from Table 1 and instead modify η. The results are presented in Figure 7.

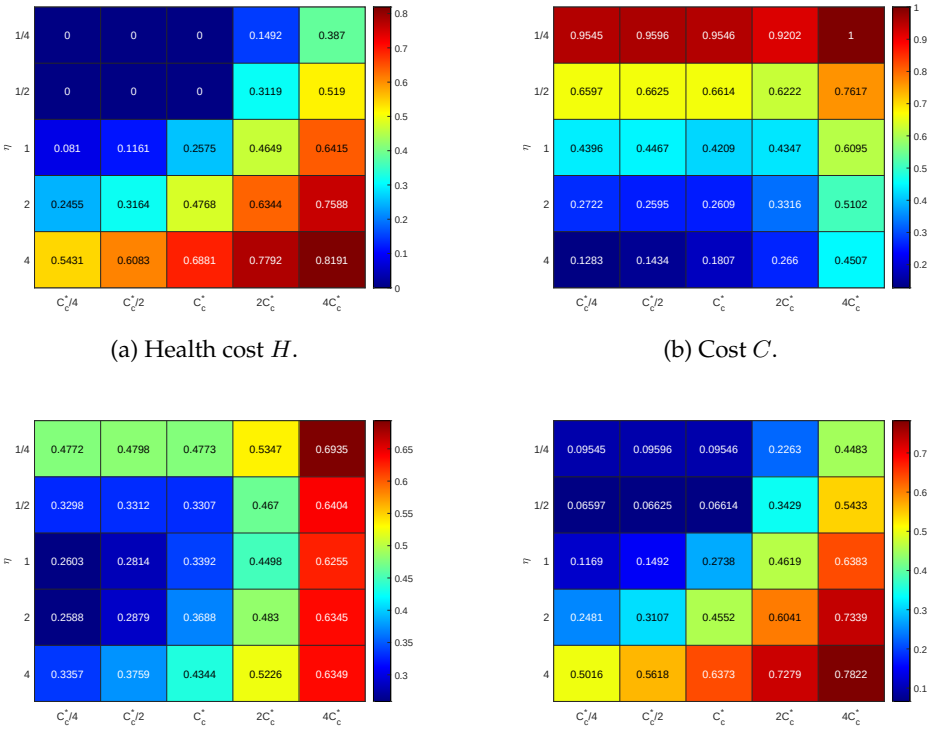

(a) Health cost H.

(b) Cost C.

(c) Total cost C_T (50/50 weighting).

(d) Total cost C_T (90/10 weighting).

Figure 7: Health, cost, and total cost from varying η and C_c in the model (A 1) with other parameters fixed from Table 1 (excluding C_0 which is appropriately updated with C_c). C_C^* refers to the base values in Table 1. In these simulations $H_\infty = 292.7$ and $C_\infty = 614$ days.

Figure 7b shows a different result compared to the case of Figure 3b when (2.4) was used for the relaxation. In the latter case, there was a general trend upward in cost that had little difference between the value of M_c, however in Figure 7b there is a strong dependence in η. This is because the multi-secondary outbreaks caused by reducing relaxation with high active cases extends the duration of the epidemic which only increases the cumulative cost. The high impact of this is noticed as well with $C_\infty = 230$ days for Figure 3 while $C_\infty = 614$ days for Figure 7. H_∞ remains the same in both cases since that is calculated with no social distancing at all (and therefore no social relaxation).

The introduction of the modified relaxation cost (3.1) has an impact on the health cost as seen in Figure 7a where a seemingly strange result is that increasing spending leads to worse health outcomes. This is particularly interesting for a case such as $\eta = 1/4$ and $C_c = C_c^*$ as there is no healthcare cost, i.e. the tested active cases never surpasses the critical threshold. However, spending four times as much to encourage people to stay home leads to a significantly higher healthcare cost. The rationale for this is similar to what was observed in [31] where keeping people isolated for a longer duration increases their fatigue and resistance to staying isolated in future instances. Figures 7c and 7d demonstrate the impact of this fatigue since regardless of weighting to health cost, the cheapest total cost options are with minimal encouragement to isolate. However, for a given cost, a higher reactivity (smaller η) to active cases does not lead to a minimum total cost. This is because there is a critical value of η below which no additional healthcare savings occur but increasing expenses occur for relaxation. These results suggest a careful policy direction with more lock-downs of shorter duration.

The plots of cases and total infections for each of the scenarios in Figure 7 can be found in the supplementary material. We plot the cumulative symptomatic-infected proportions for each scenario in Figure 8.

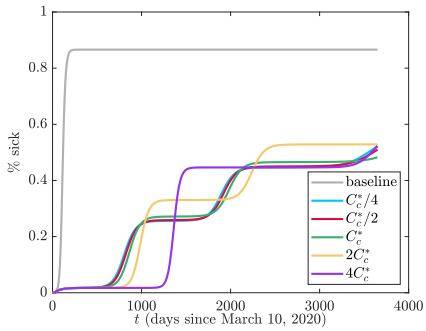

(a) $\eta = 1/4$.

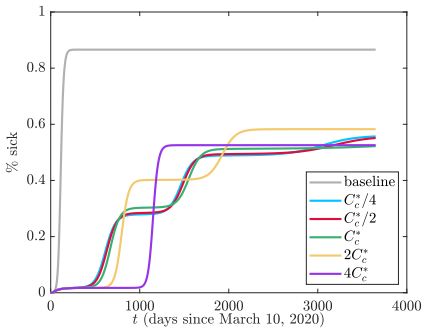

(b) $\eta = /2$.

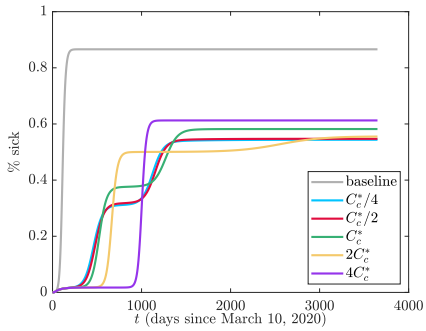

(c) $\eta = 1$.

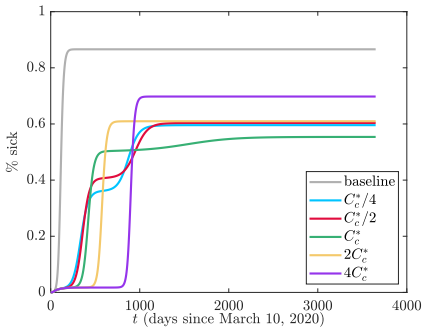

(d) $\eta = 2$.

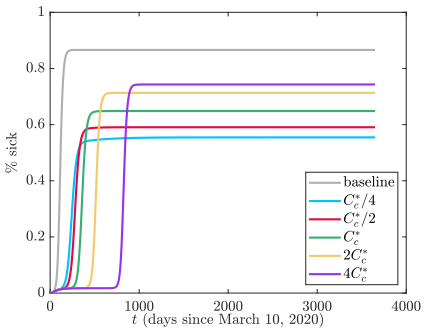

(e) $\eta = 4$.

Figure 8: Total cumulative symptomatic cases (plotted as a percentage of the total population) with the modified cost function (3.1). The baseline case refers to no social distancing, i.e. $\mu_{\max} = 0$.

Unlike the scenarios in Figure 5 associated with the relaxation cost (2.4), basing relaxation on active cases as well can impact the terminal number of cumulative infections. Continually reducing η decreases the total number of infected people which provides more evidence that increasing the relaxation cost threshold C_c can cause more people to become infected. However

similar to Figure 5, increasing C_c leads to a longer delay before significant infection numbers occur.

4. Conclusion

We have presented a model for COVID-19 that allows for dynamic social distancing and relaxation based on the measured active cases and individual cost of isolating. The aim of this approach is that it more accurately reflects human behaviour and psychology unlike the modelling approach where behaviours are turned on and off at pre-determined times. Understanding how people will react to a change in policy surrounding lock-downs or bans on social gatherings is essential in gauging the impact that COVID-19 and mitigation strategies will have on infections and mortality. Improving this modelling aspect can make sure that policies are put into place at the right time so people will react accordingly.

By modelling behaviour dynamically we were able to produce unintuitive results regarding the relative total cost of the disease, namely that increasing vigilance and relaxation cost as well as decreasing reactivity to growing case loads does not necessarily lead to a decrease in total cost. This is because of the desire for people to socialize and fatigue for being intrinsically part of the model. We have demonstrated that in certain circumstances the additional healthcare cost can be eliminated entirely, but at a relatively large cost to keeping people home.

An advantage of the dynamic framework used in this model is that it is not restricted to Ontario nor is it even restricted to COVID-19. Changing the disease and behaviour parameters will allow this model to adapt to other scenarios. For COVID-19, policy makers would be advised to use data such as that used here from [25] in the relatively early stages of a lock-down to fit behaviour parameters. Earlier time point data helps reduce the likelihood that the relaxation cost threshold has been exceeded so that the behaviour parameters are more accurate. Otherwise, k_c^* and M_c^* become stronger functions of the choice for C_c^*. The limited data and types of data available should discourage too much parameter fitting. Having determined the parameters to a given set of data, cost analysis using (2.7) can be done leading to results similar to Figures 3 and 7. Understanding the influence of tangible actions such as forced closures, wage subsidies, etc. on parameters such as M_c, C_c, and η likely requires surveys and other followup studies.

It is important to acknowledge that this model does not take into account vaccination or other pharmaceutical interventions. These have an important role in not only limiting the healthcare impact, but also in outbreak peak time and duration. The introduction of the modified cost in (3.1) causes significant delays between peaks at increased economic and psychological cost. The duration of the pandemic can then be several years longer than when fatigue is strong resulting in a single outbreak peak. The duration may be significantly longer than the time for an effective vaccine to be developed and deployed and this needs to be considered in future work. Another important consideration is that social distancing is not truly discrete in that people do not suddenly reduce their contacts. In reality it is a spectrum with fluid contact rates and this needs to be further explored. Finally, taking the testing rates constant should be relaxed and reflect that both the testing capacity and willingness for individuals to test is a function of disease progression.

Acknowledgements. The authors are grateful to members from the Centre for Disease Modelling for feedback on the model. We thank Suzan Sardroodi for a thorough review of the manuscript.

Funding. IRM acknowledges funding from an NSERC Discovery grant (2019-06337). JMH acknowledges funding from an NSERC Discovery grant and Discovery Accelerator Supplement.

A. Differential Equation Model

The differential equation model visualized in Figure 1 is given by

$$
\begin{aligned}
\dot{S}_0 =& - F_{S_0} - \mu_{S_0S_1}S_0 - \mu_{S_0S_2}S_0 + \nu_{S_1S_0}S_1 + \nu_{S_2S_0}S_2 \\
\dot{S}_1 =& - F_{S_1} - \mu_{S_1S_2}S_1 + \mu_{S_0S_1}S_0 - \nu_{S_1S_0}S_1 + \nu_{S_2S_1}S_2 \\
\dot{S}_2 =& \mu_{S_0S_2}S_0 + \mu_{S_1S_2}S_1 - \nu_{S_2S_0}S_2 - \nu_{S_2S_1}S_2 \\
\dot{E}_0 =& F_{S_0} - \mu_{E_0E_1}E_0 - \mu_{E_0E_2}E_0 + \nu_{E_1E_0}E_1 + \nu_{E_2E_0}E_2 - \sigma E_0 \\
\dot{E}_1 =& F_{S_1} - \mu_{E_1E_2}E_1 + \mu_{E_0E_1}E_0 - \nu_{E_0E_1}E_1 + \nu_{E_2E_1}E_2 - \sigma E_1 \\
\dot{E}_2 =& \mu_{E_0E_2}E_0 + \mu_{E_1E_2}E_1 - \nu_{E_2E_0}E_2 - \nu_{E_2E_1}E_2 - \sigma E_2 \\
\dot{P}_0 =& \sigma E_0 - \mu_{P_0P_1}P_0 - \mu_{P_0P_2}P_0 + \nu_{P_1P_0}P_1 + \nu_{P_2P_0}P_2 - \phi P_0 - \rho_A P_0 \\
\dot{P}_1 =& \sigma E_1 - \mu_{P_1P_2}P_1 + \mu_{P_0P_2}P_0 - \nu_{P_1P_0}P_1 + \nu_{P_2P_1}P_2 - \phi P_1 - \rho_A P_1 \\
\dot{P}_2 =& \sigma E_2 + \mu_{P_0P_2}P_0 + \mu_{P_1P_2}P_1 - \nu_{P_2P_0}P_2 - \nu_{P_2P_1}P_2 - \phi P_2 - \rho_A P_2 \\
\dot{P}_M =& \rho_A(P_0 + P_1 + P_2) - \phi P_M \\
\dot{I}_{S_0} =& q\phi P_0 - \mu_{I_{S_0}I_{S_1}}I_{S_0} - \mu_{I_{S_0}I_{S_2}}I_{S_0} - \gamma_S I_{S_0} - \rho_S I_{S_0} \\
\dot{I}_{S_1} =& q\phi P_1 + \mu_{I_{S_0}I_{S_1}}I_{S_0} - \mu_{I_{S_1}I_{S_2}}I_{S_1} - \gamma_S I_{S_1} - \rho_S I_{S_1} \\
\dot{I}_{S_2} =& q\phi P_2 + \mu_{I_{S_0}I_{S_2}}I_{S_0} + \mu_{I_{S_1}I_{S_2}}I_{S_1} - \gamma_S I_{S_2} - \rho_S I_{S_2} \\
\dot{I}_{S_M} =& \rho_S(I_{S_0} + I_{S_1} + I_{S_2}) + q\phi P_M - \gamma_S I_{S_M} \\
\dot{I}_{A_0} =& (1-q)\phi P_0 - \mu_{I_{A_0}I_{A_1}}I_{A_0} - \mu_{I_{A_0}I_{A_2}}I_{A_0} + \nu_{I_{A_1}I_{A_0}}I_{A_1} + \nu_{I_{A_2}I_{A_0}}I_{A_2} - \gamma_A I_{A_0} - \rho_A I_{A_0} \\
\dot{I}_{A_1} =& (1-q)\phi P_1 - \mu_{I_{A_1}I_{A_2}}I_{A_1} + \mu_{I_{A_0}I_{A_1}}I_{A_0} - \nu_{I_{A_1}I_{A_0}}I_{A_1} + \nu_{I_{A_2}I_{A_1}}I_{A_2} - \gamma_A I_{A_1} - \rho_A I_{A_1} \\
\dot{I}_{A_2} =& (1-q)\phi P_2 + \mu_{I_{A_0}I_{A_2}}I_{A_0} + \mu_{I_{A_1}I_{A_2}}I_{A_1} - \nu_{I_{A_0}I_{A_2}}I_{A_2} - \nu_{I_{A_2}I_{A_1}}I_{A_2} - \gamma_A I_{A_2} - \rho_A I_{A_2} \\
\dot{I}_{A_M} =& \rho_A(I_{A_0} + I_{A_1} + I_{A_2}) + (1-q)\phi P_M - \gamma_A I_{A_M} \\
\dot{R}_{S_0} =& \gamma_S I_{S_0} \\
\dot{R}_{S_1} =& \gamma_S I_{S_1} \\
\dot{R}_{S_2} =& \gamma_S I_{S_2} \\
\dot{R}_{S_M} =& \gamma_S I_{S_M} \\
\dot{R}_{A_0} =& \gamma_A I_{A_0} \\
\dot{R}_{A_1} =& \gamma_A I_{A_1} \\
\dot{R}_{A_2} =& \gamma_A I_{A_2} \\
\dot{R}_{A_M} =& \gamma_A I_{A_M}
\end{aligned}
\tag{A 1}
$$

where F_{s_i} is the force of infection,

$$
F_{S_0} = \frac{N_{\text{crit}}}{N}\left(\beta_{S_0P_0}S_0P_0 + \beta_{S_0I_{S_0}}S_0I_{S_0} + \beta_{S_0I_{A_0}}S_0I_{A_0} + \beta_{S_0P_1}S_0P_1 + \beta_{S_0I_{S_1}}S_0I_{S_1} + \beta_{S_0I_{A_1}}S_0I_{A_1}\right) \tag{A 2a}
$$

$$
F_{S_1} = \frac{N_{\text{crit}}}{N}\left(\beta_{S_1P_0}S_1P_0 + \beta_{S_1I_{S_0}}S_1I_{S_0} + \beta_{S_1I_{A_0}}S_1I_{A_0} + \beta_{S_1P_1}S_1P_1 + \beta_{S_1I_{S_1}}S_1I_{S_1} + \beta_{S_1I_{A_1}}S_1I_{A_1}\right), \tag{A 2b}
$$

In deriving the model we have normalized the population by N_{crit} which represents the population that causes the healthcare system to be at capacity.

B. Parameter Fitting and Model Sensitivity

Many of the parameters associated with the natural progression of the disease are unknown as are several of the intervention parameters such as social distancing and testing. We use data from [25] for the 161 days between March 10 and August 18, 2020 on active and total cases to elucidate some key parameters. To do this we solve our model (A 1) with the parameters in Table 1 excluding k_c, k_0, M_c, M_0, ρ_A and ρ_S which we fit to the data. We run our model for 161 days using an initial condition that 0.02% of the population was initially infected with the remaining 99.98% being symptomatic. The actual number of people with COVID-19 is a matter of speculation and the arbitrary choice of the initial value will affect the fitting parameters, particularly the testing rates which are intimately linked. We do not partition any of the initial infected population into symptomatic or asymptomatic also due to the lack of clarity on true numbers. To help constrain the model we take $k_0 = 4k_c$ so that the doubling rate has to double twice to trigger the half-maximal social distancing. We also take $M_0 = 2M_c$ so that the number of active cases need to double to trigger the half-maximal social distancing rate. Finally, since we assume that symptomatic people are more likely to get tested than asymptomatic people we take $\rho_S = 4\rho_A$. These constraints should not be too restricting, likely impacting the fitted values of the remaining free variables k_c, M_c, and ρ_A.

We use a non-linear least squares iterative procedure to identify the parameters. This leads to the values k_c=1/16.24 d^{-1}, $M_c = 2.57 \times 10^{-2}$, and $\rho_A = 8.7 \times 10^{-3}$ d^{-1} as in Table 1 with a residual norm of 9.5×10^{-3}. A graphical representation of the fit between data and model is in Figure 2.

(a) Sensitivity Analysis

Having fit data to the model we then performed a sensitivity analysis on the parameters ρ_S, ρ_A, q_I, μ_I, q_2, q_0, q, γ, ϕ, σ, and α. We used Table 1 for the fixed parameters and as mean values for the varying parameters, each distributed uniformly between maximum and minimum values. We used the latin hypercube sampling technique with 10000 iterations and a Spearman partial rank correlation coefficient to measure monotonicity. We tested the sensitivity to the cumulative infected (symptomatic and asymptomatic), susceptibles, peak time for the outbreak, and the value at the peak of the outbreak. We plot the results in Figure 9

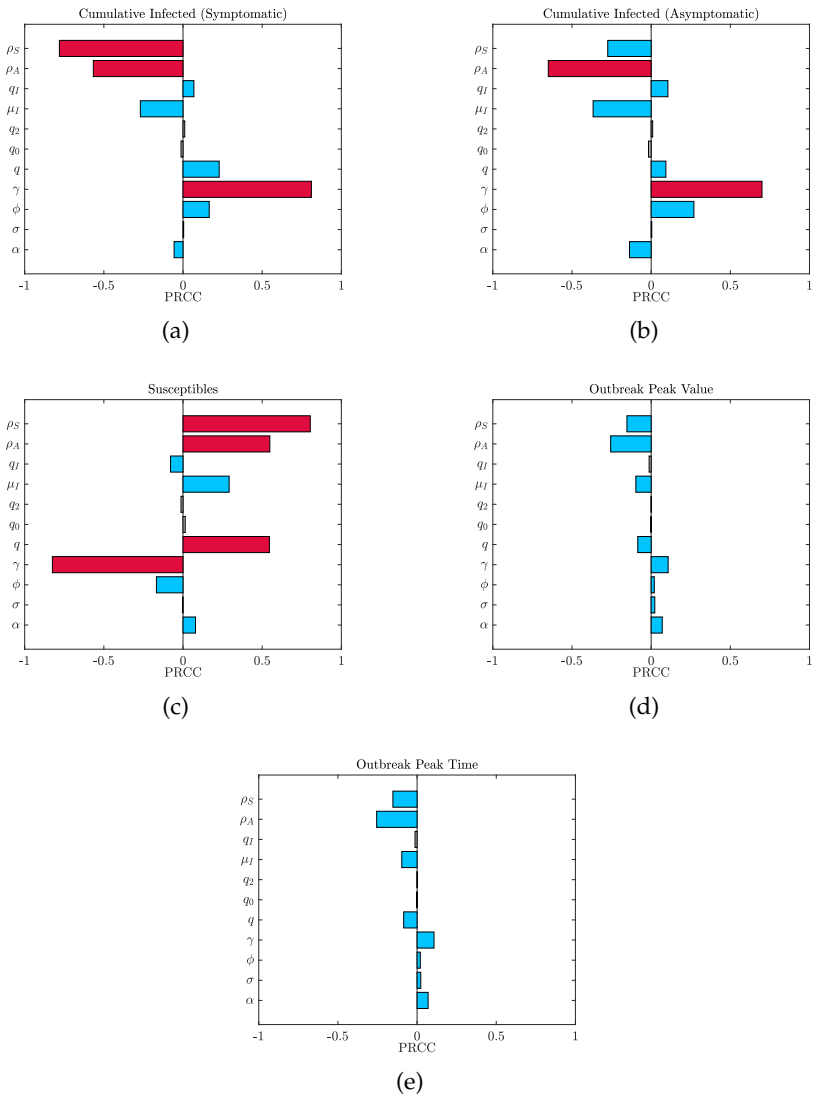

Figure 9: Sensitivity analysis of the model (A 1) using 10000 iterations of a latin hypercube sampling method with a Spearman partial rank correlation coefficient. Grey bars indicate a parameter with a p-value $p > 0.05$ dismissing their significance. If $p < 0.05$ the bar is blue unless it is strongly correlated (absolute PRCC greater that 0.5) in which case it is red.

The most significant parameter is the recovery rate γ (assumed the same for both classes) which seemingly has inverse behaviour to what is expected. That is an increase in the recovery rate seems to cause more people to become sick. This is because the basic reproduction number is fixed at 2.4 and therefore changing γ effectively changes the transmission β making a higher recovery rate lead to a more transmissible disease. Aside from this, the most significant parameters unsurprisingly are the testing rates ρ_S and ρ_A as well as the symptomatic proportion q. This supports the importance of testing and social distancing. Interestingly, there is not much sensitivity to the peak time and value of the outbreak confirming the need for long-term planning regarding vaccination and hospital resource management.

We did not perform a sensitivity analysis on k_c or M_c as these are policy parameters. Their sensitivity is effectively measured by comparing costs in Figures 3 and 7.

References

1. Kucharski, A. J., Russell, T. W., Diamond, C., Liu, Y., Edmunds, J., Funk, S., Eggo, R. M., Sun, F., Jit, M., Munday, J. D., et al. (2020). Early dynamics of transmission and control of covid-19: a mathematical modelling study. *The lancet infectious diseases*.
2. Ndairou, F., Area, I., Nieto, J. J., and Torres, D. F. (2020). Mathematical modeling of covid-19 transmission dynamics with a case study of wuhan. *Chaos, Solitons & Fractals*, page 109846.
3. Accounttemps (2019). 9 in 10 employees come to work sick, survey shows. survey details retrieved on September 29, 2020 from http://rh-us.mediaroom.com/2019-10-24-9-In-10-Employees-Come-To-Work-Sick-Survey-Shows.
4. Atkeson, A. (2020). What will be the economic impact of covid-19 in the us? rough estimates of disease scenarios. Technical report, National Bureau of Economic Research.
5. Böhmer, M. M., Buchholz, U., Corman, V. M., Hoch, M., Katz, K., Marosevic, D. V., Böhm, S., Woudenberg, T., Ackermann, N., Konrad, R., et al. (2020). Investigation of a covid-19 outbreak in germany resulting from a single travel-associated primary case: a case series. *The Lancet Infectious Diseases*.
6. Campbell, K. H., Tornatore, J. M., Lawrence, K. E., Illuzzi, J. L., Sussman, L. S., Lipkind, H. S., and Pettker, C. M. (2020). Prevalence of sars-cov-2 among patients admitted for childbirth in southern connecticut. *Jama*.
7. Collinson, S., Khan, K., and Heffernan, J. M. (2015). The effects of media reports on disease spread and important public health measurements. *PloS one*, 10(11):e0141423.
8. Cui, J., Sun, Y., and Zhu, H. (2008). The impact of media on the control of infectious diseases. *Journal of dynamics and differential equations*, 20(1):31–53.
9. Diekmann, O., Heesterbeek, J., and Roberts, M. G. (2010). The construction of next-generation matrices for compartmental epidemic models. *Journal of the Royal Society Interface*, 7(47):873–885.
10. Ferguson, N., Laydon, D., Nedjati-Gilani, G., Imai, N., Ainslie, K., Baguelin, M., Bhatia, S., Boonyasiri, A., Cucunubá, Z., Cuomo-Dannenburg, G., et al. (2020). Impact of non-pharmaceutical interventions (npis) to reduce covid-19 mortality and healthcare demand. imperial college covid-19 response team.
11. Ghinai, I., Woods, S., Ritger, K. A., McPherson, T. D., Black, S. R., Sparrow, L., Fricchione, M. J., Kerins, J. L., Pacilli, M., Ruestow, P. S., et al. (2020). Community transmission of sars-cov-2 at two family gatherings—chicago, illinois, february–march 2020. Technical report, Center for Disease Control.
12. Heffernan, J. M., Smith, R. J., and Wahl, L. M. (2005). Perspectives on the basic reproductive ratio. *Journal of the Royal Society Interface*, 2(4):281–293.
13. Hethcote, H. W. (2000). The mathematics of infectious diseases. *SIAM review*, 42(4):599–653.
14. Ivorra, B., Ferrández, M. R., Vela-Pérez, M., and Ramos, A. (2020). Mathematical modeling of the spread of the coronavirus disease 2019 (covid-19) taking into account the undetected infections. the case of china. *Communications in nonlinear science and numerical simulation*, page 105303.
15. Kermack, W. O. and McKendrick, A. G. (1927). A contribution to the mathematical theory of epidemics. *Proceedings of the royal society of london. Series A, Containing papers of a mathematical and physical character*, 115(772):700–721.
16. Kissler, S. M., Tedijanto, C., Goldstein, E., Grad, Y. H., and Lipsitch, M. (2020a). Projecting the transmission dynamics of sars-cov-2 through the postpandemic period. *Science*, 368(6493):860–868.
17. Kissler, S. M., Tedijanto, C., Lipsitch, M., and Grad, Y. (2020b). Social distancing strategies for curbing the covid-19 epidemic. *medRxiv*.
18. Mahajan, A., Solanki, R., and Sivadas, N. (2020). Estimation of undetected symptomatic and asymptomatic cases of covid-19 infection and prediction of its spread in usa. *medRxiv*.

19. Matrajt, L. and Leung, T. (2020). Evaluating the effectiveness of social distancing interventions to delay or flatten the epidemic curve of coronavirus disease. *Emerging infectious diseases*, 26(8):1740.
20. McBryde, E. S., Meehan, M. T., Adegboye, O. A., Adekunle, A. I., Caldwell, J. M., Pak, A., Rojas, D. P., Williams, B., and Trauer, J. M. (2020). Role of modelling in covid-19 policy development. *Paediatric Respiratory Reviews*.
21. Mizumoto, K. and Chowell, G. (2020). Transmission potential of the novel coronavirus (covid-19) onboard the diamond princess cruises ship, 2020. *Infectious Disease Modelling*, 5:264 – 270.
22. Nicola, M., Alsafi, Z., Sohrabi, C., Kerwan, A., Al-Jabir, A., Iosifidis, C., Agha, M., and Agha, R. (2020). The socio-economic implications of the coronavirus pandemic (covid-19): A review. *International journal of surgery (London, England)*, 78:185.
23. Patel, M. C., Chaisson, L. H., Borgetti, S., Burdsall, D., Chugh, R. K., Hoff, C. R., Murphy, E. B., Murskyj, E. A., Wilson, S., Ramos, J., et al. (2020). Asymptomatic sars-cov-2 infection and covid-19 mortality during an outbreak investigation in a skilled nursing facility. *Clinical Infectious Diseases*.
24. Petersen, E., Koopmans, M., Go, U., Hamer, D. H., Petrosillo, N., Castelli, F., Storgaard, M., Al Khalili, S., and Simonsen, L. (2020). Comparing sars-cov-2 with sars-cov and influenza pandemics. *The Lancet Infectious Diseases*.
25. Public Health Ontario (2020). COVID19 data. data retrieved on August 18, 2020 from https://data.ontario.ca/dataset/status-of-covid-19-cases-in-ontario.
26. Russell, T. W., Golding, N., Hellewell, J., Abbott, S., Wright, L., Pearson, C. A., van Zandvoort, K., Jarvis, C. I., Gibbs, H., Liu, Y., et al. (2020). Reconstructing the early global dynamics of under-ascertained covid-19 cases and infections. *medRxiv*.
27. Sakurai, A., Sasaki, T., Kato, S., Hayashi, M., Tsuzuki, S.-i., Ishihara, T., Iwata, M., Morise, Z., and Doi, Y. (2020). Natural history of asymptomatic sars-cov-2 infection. *New England Journal of Medicine*.
28. Sánchez-Álvarez, J. E., Fontán, M. P., Martín, C. J., Pelícano, M. B., Reina, C. J. C., Prieto, Á. M. S., Melilli, E., Barrios, M. C., Heras, M. M., o lores del Pino, M. D., et al. (2020). Status of sars-cov-2 infection in patients on renal replacement therapy report of the covid-19 registry of the spanish society of nephrology (sen). *Nefrología (English Edition)*.
29. Steensels, D., Oris, E., Coninx, L., Nuyens, D., Delforge, M.-L., Vermeersch, P., and Heylen, L. (2020). Hospital-wide sars-cov-2 antibody screening in 3056 staff in a tertiary center in belgium. *Jama*, 324(2):195–197.
30. Tchuenche, J. M., Dube, N., Bhunu, C. P., Smith, R. J., and Bauch, C. T. (2011). The impact of media coverage on the transmission dynamics of human influenza. *BMC Public Health*, 11(S1):S5.
31. Tuite, A. R., Fisman, D. N., and Greer, A. L. (2020). Mathematical modelling of covid-19 transmission and mitigation strategies in the population of ontario, canada. *CMAJ*, 192(19):E497–E505.
32. Wolfel, R., Corman, V., Guggemos, W., et al. (2020). Virological assessment of hospitalized cases of coronavirus disease 2019. *medRxiv preprint* https://www.medrxiv.org/content/10.1101/2020.03, 5:v1.
33. Xiao, Y., Tang, S., and Wu, J. (2015). Media impact switching surface during an infectious disease outbreak. *Scientific reports*, 5:7838.
34. Yuan, P., Li, J., Aruffo, E., Li, Q., Zheng, T., Ogden, N., Sander, B., Heffernan, J., Gatov, E., Gournis, E., Collier, S., Tan, Y., Li, J., Arino, J., Bélair, J., Watmough, J., Kong, J. D., Moyles, I., and Zhu, H. (2020). Efficacy of "stay-at-home" policy and transmission of covid-19 in toronto, canada: a mathematical modeling study. *CMAJ Open*. Submitted.